Supporting Information

Hydrophobic Surface Efficiently Boosting Cu_2O Nanowires Photoelectrochemical CO_2 Reduction Activity

Yanfang Zhang, [a] Weixin Qiu, [a] Yang Liu, [a] Keke Wang, [a] Luwei Zou, [b] Yu Zhou, [b] Min Liu, [b] Xiaoqing Qiu, [a] Jie Li, [a*] Wenzhang Li [a,c*]

[a] School of Chemistry and Chemical Engineering, Central South University, Changsha, 410083, China

[b] School of Physics and Electronics, Central South University, Changsha 410083, China

[c] Hunan Provincial Key Laboratory of Chemical Power Sources, Central South University, Changsha, 410083, China

* Corresponding authors.

E-mail addresses: liwenzhang@csu.edu.cn (Wenzhang Li), lijieliu@csu.edu.cn (Jie Li).

Contents

c) Cu_2O/Sn/PTFE. d) IMPS plots of Cu_2O, Cu_2O/Sn and Cu_2O/Sn/PTFE.

Figure S16. The product Faradaic efficiency of Cu_2O/Sn/PTFE at different pH electrolytes (-0.7 V vs. RHE).

Tables

Table S1. The contents of each component in Cu_2O/Sn/PTFE photoelectrode.

Table S2. Performance comparison of recent reports about Cu_2O photocathode for PEC CO_2RR.

Table S3. Physical resistance (R_1), charge transfer resistance (R_{ct}) and charge transfer efficiency of the photoelectrode.

Experiment section

Preparation of Cu_2O NWs Photocathode

First, $Cu(OH)_2$ NWs were synthesized by anodizing in a two-electrode device. The polished copper foil was used as the working electrode, and the platinum sheet was used as the counter electrode, anodized in 3 M potassium hydroxide solution (3 M KOH) at a constant current of 10 mA/cm^2 for 8 min to obtain blue $Cu(OH)_2$ NWs. Then, the as-prepared $Cu(OH)_2$ NWs were calcined at 180 °C for 1 h to convert to CuO. Finally, the Cu_2O NWs were obtained by annealing at 600 °C for 4 h in an Ar flowing atmosphere.

Preparation of Cu_2O/Sn Photocathodes

The Cu_2O/Sn photocathode was synthesized by depositing 10 nm metal Sn on the Cu_2O NWs photocathode by physical vapor deposition (PVD). The metal tin with a purity of 99.9% was used as the Sn source, and the evaporation rate was controlled to be 0.1 Å·s^{-1}.

Preparation of Cu_2O/Sn/PTFE Photocathode

The surface of Cu_2O/Sn electrode was further modified with PTFE (Poly tetra fluoroethylene) by dipping method to obtain Cu_2O/Sn/PTFE photoelectrode. First, the 60 wt.% PTFE emulsion was diluted with water to obtain the desired weight percent (1%, 5%, 10%, 15% and 20%) of the PTFE emulsion, and ultrasonically dispersed it uniformly. Next, the Cu_2O/Sn photocathodes were immersed in PTFE emulsions with different weight percent for different times to obtain the corresponding Cu_2O/Sn/PTFE photoelectrodes. The photocathodes obtained by immersion in different weight percent

of PTFE emulsion for 1 min were named Cu_2O/Sn/PTFE-1, Cu_2O/Sn/PTFE, Cu_2O/Sn/PTFE-10, Cu_2O/Sn/PTFE-15 and Cu_2O/Sn/PTFE-20, respectively. The photocathode obtained by dipping in 5 wt.% PTFE emulsion for 20 s, 40 s, 1 min, 3 min, 5 min are named Cu_2O/Sn/PTFE-20 s, Cu_2O/Sn/PTFE-40 s, Cu_2O/Sn/PTFE-1min, Cu_2O/Sn/PTFE-3min and Cu_2O/Sn/PTFE-5min, respectively.

Morphology and structure characterization

The crystal structures of the samples were recorded by X-ray diffractometer (XRD, D/Max2250, Rigaku) using Cu Kα as radiation source (λ = 0.15406 nm). Fourier transform infrared (FT-IR) spectra were collected on a Nicolet 6700 FT-IR spectrometer (Thermo, MA, USA) with the recorded wavenumbers from 400 to 4000 cm^{-1}. TU-1901 UV-vis spectrophotometer with integrating sphere was used to record ultraviolet-visible absorption (UV-vis) spectra for analysis of optical properties. The contact angle (CA) of water (10 μL) was determined using an OCA 20 instrument (Dataphysics, Germany). All CA images were collected within 0.5 min after water droplet being placed on the samples surface. Scanning electron microscopy (Nova Nano SEM 230, FEI) and high-resolution transmission electron microscopy (HRTEM, Tecnai G2 F20, FEI) were used to record the surface topography of the samples. X-ray photoelectron spectroscopy (XPS, Thermo Scientific K-Alpha$_+$) with an Al-Kα source was used to determine the elemental composition and valence state of the samples.

Photoelectrochemical measurements and CO_2 reduction performance

PEC measurements were performed using an electrochemical workstation (Zahner) under AM 1.5 G illumination (100 mW cm^{-2}). An H-type quartz cell was used,

isolated by a Nafion 117 proton exchange membrane, and the electrolyte was 0.1 M $KHCO_3$ solution. Before the PEC CO_2RR, CO_2 (99.99%) was purged from the electrolyte in the cathodic compartment for 30 min. The prepared photocathode, platinum sheet and Ag/AgCl electrode were used as working electrode, counter electrode and reference electrode, respectively. Linear sweep voltammetry (LSV) was performed at a scan rate of 20 mV/s over a potential range of 0.2 V to -1.6 V vs. Ag/AgCl. The PEC CO_2RR product tests were performed at different potentials (-1.0, -1.1, -1.2, -1.3, -1.4 V vs. Ag/AgCl). The CO_2 reduction products were analyzed by gas chromatograph (GC8860, Agilent, USA) and ^1H NMR spectroscopy (HPLC, Agilent, USA).

Mott-Schottky (M-S) plots were recorded at different frequencies (1, 2, 3 kHz) over the potential range of 0 to -0.2 V vs. Ag/AgCl in the dark. Open circuit potential (OCP) was recorded under chopping illumination with 60 s light-on and 30 s light-off. Electrochemical impedance spectroscopy (EIS) was measured at -1.3 V vs. Ag/AgCl over a frequency range of 10 kHz to 100 mHz with an AC amplitude of 10 mV. Cyclic voltammetry (CV) curves were measured at different scan rates (20, 40, 60, 80, 100 mV s-1) from -0.15 to -0.05 V vs. Ag/AgCl. Intensity-modulated photocurrent spectroscopy (IMPS) was recorded by a Zahner CIMPS system at -0.5 V vs. Ag/AgCl over a frequency range of 5 kHz to 100 mHz. Convert the potential to a reversible hydrogen electrode (RHE) by the following formula:

$$E\ (\text{vs. RHE}) = E\ (\text{vs. Ag/AgCl}) + 0.059 \times \text{pH} + 0.197\ \text{V} \quad (1)$$

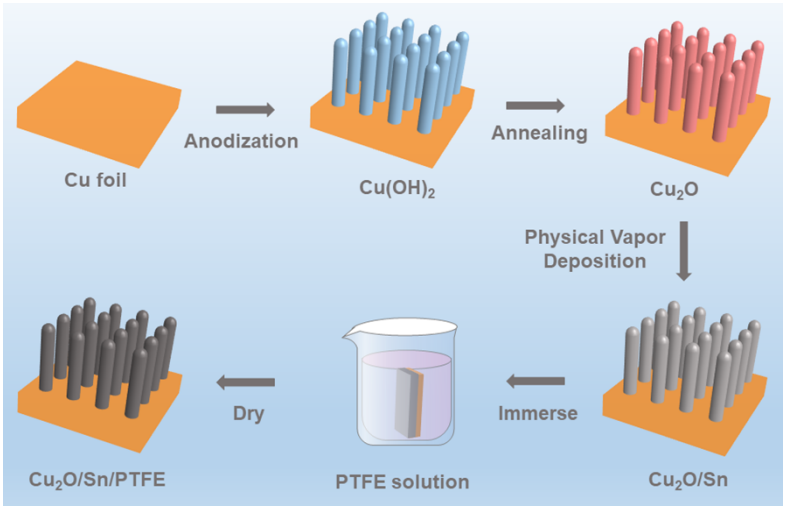

Figure S1. Illustration of the formation of Cu_2O, Cu_2O/Sn and Cu_2O/Sn/PTFE.

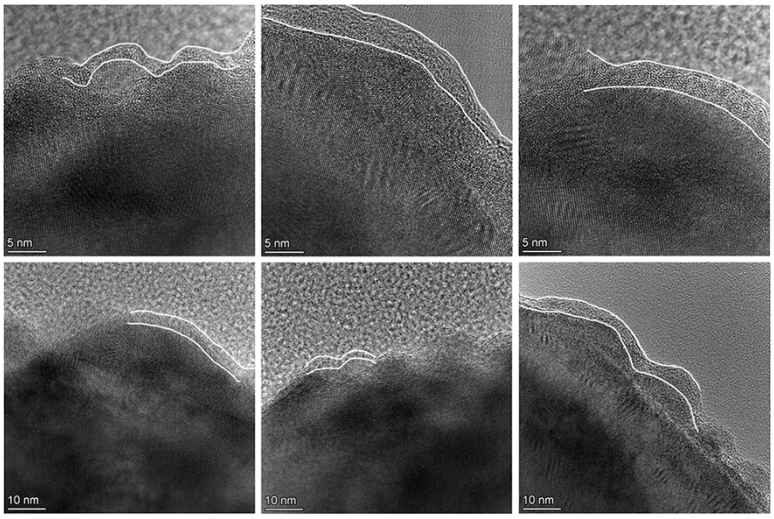

Figure S2. The HRTEM images of Cu_2O/Sn/PTFE.

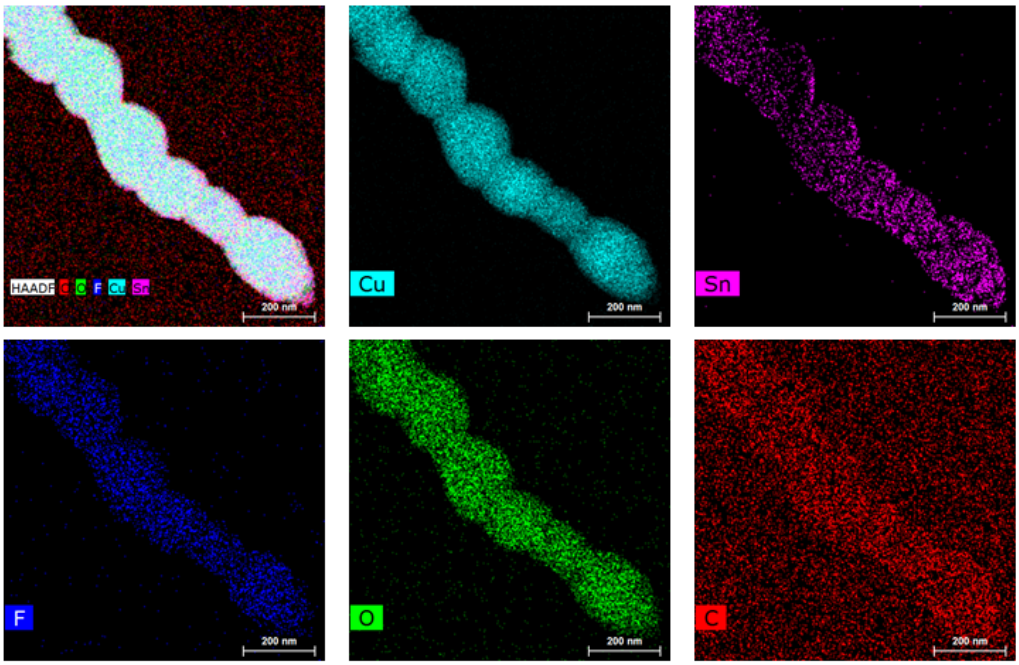

Figure S3. HAADF-STEM and EDX spectroscopy of Cu_2O/Sn/PTFE.

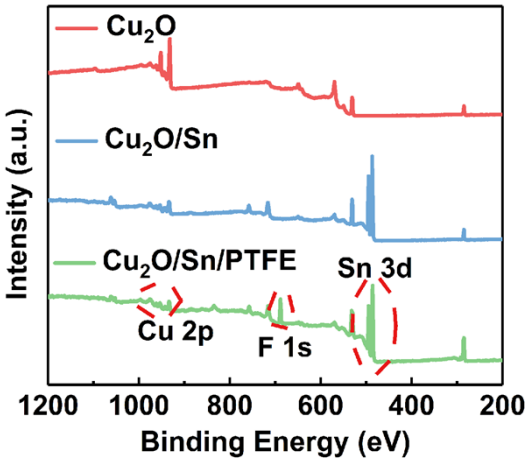

Figure S4. The XPS full spectrum of the photoelectrodes.

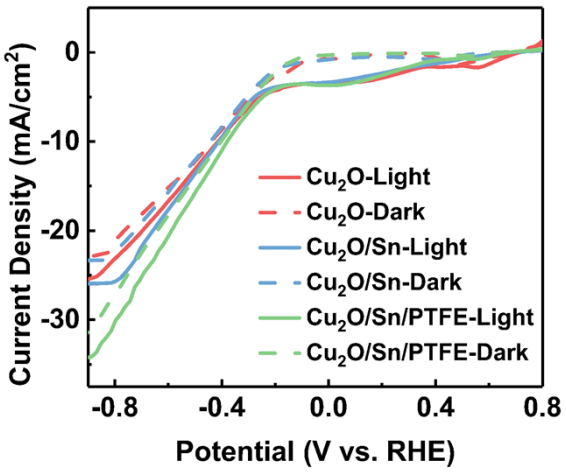

Figure S5. LSV curves of Cu_2O, Cu_2O/Sn and Cu_2O/Sn/PTFE.

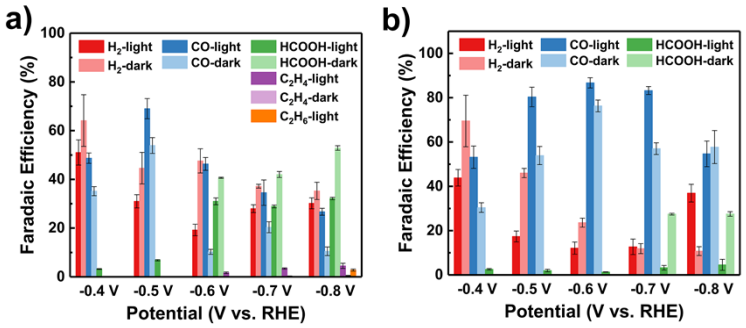

Figure S6. The product Faradaic efficiency of Cu_2O and Cu_2O/Sn at different potentials under light/dark.

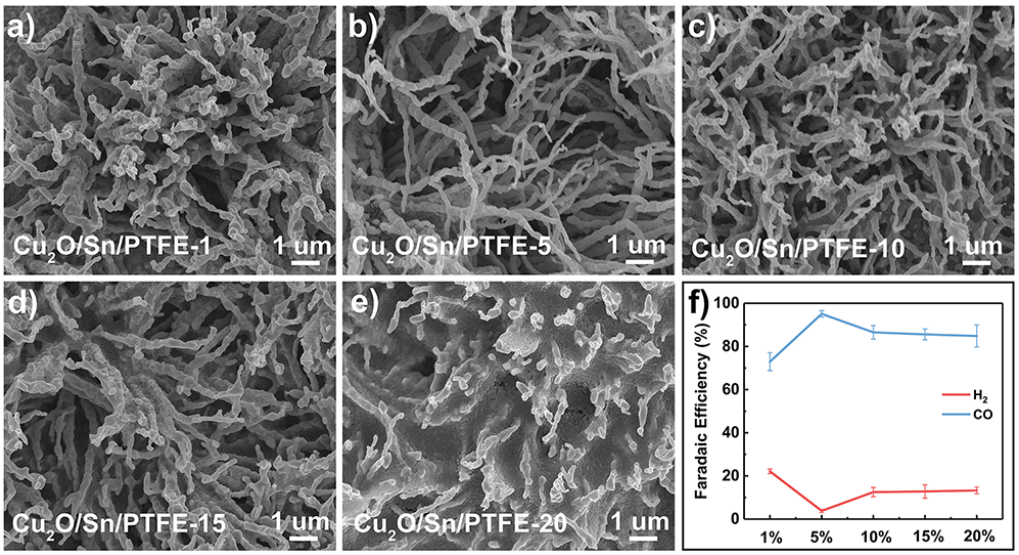

Figure S7. a)-e) SEM images of photoelectrodes after immersion in different mass fractions of PTFE emulsion. f) Product Faradaic efficiency of photoelectrodes after immersion in different mass fractions of PTFE emulsion.

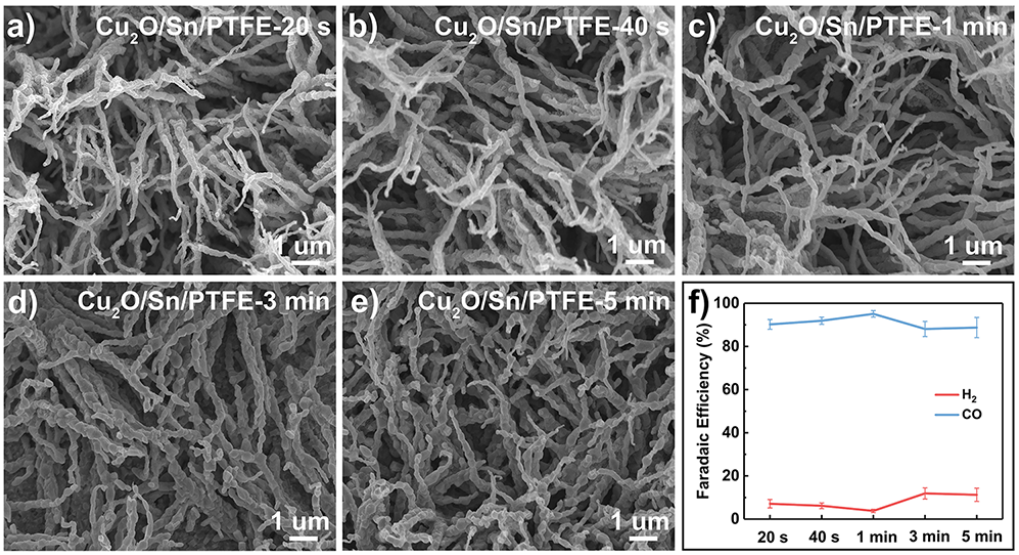

Figure S8. a)-e) SEM images of photoelectrode after soaking in 5 wt.% PTFE emulsion for different time. f) Product Faradaic efficiency of photoelectrode after soaking in 5 wt.% PTFE emulsion for different time (-0.7 V vs. RHE).

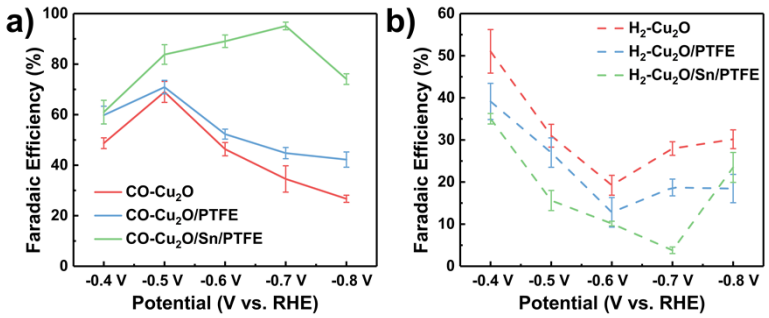

Figure S9. The product Faradaic efficiency of Cu_2O, Cu_2O/PTFE and Cu_2O/Sn/PTFE at different potentials. a) CO, b) H_2.

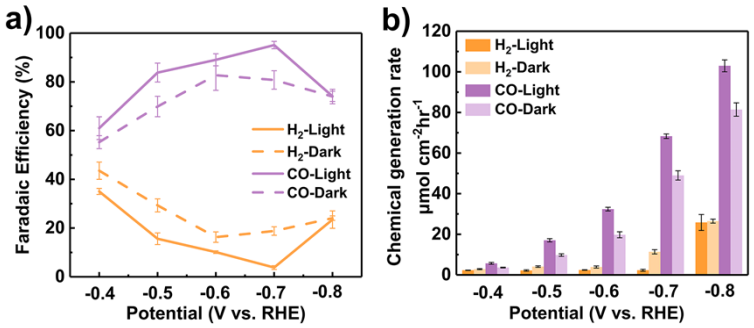

Figure S10. The comparison of faradaic efficiency and yield of Cu_2O/Sn/PTFE photocathode under illumination and in the dark at different potentials.

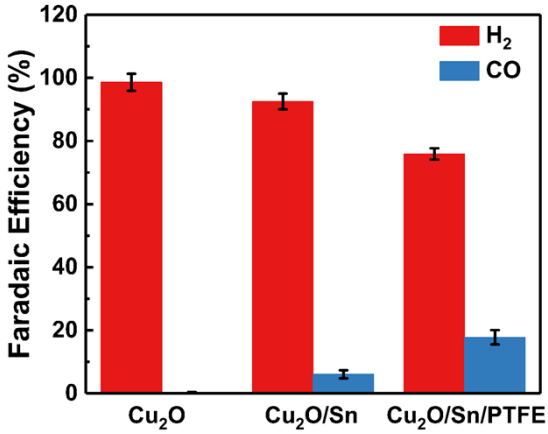

Figure S11. The product Faradaic efficiency of Cu_2O/Sn/PTFE at KPi (-0.7 V vs. RHE).

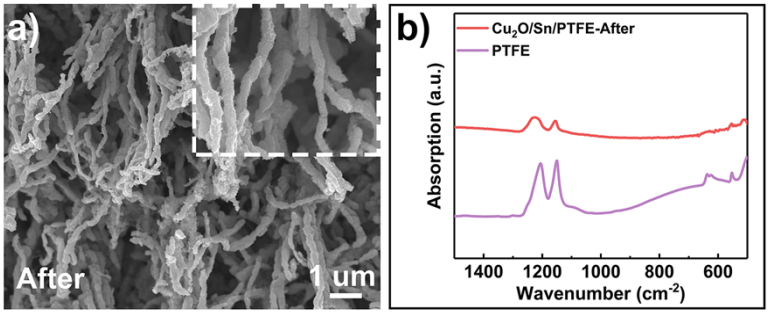

Figure S12. a) The SEM image and b) the FT-IR spectrum of Cu_2O/Sn/PTFE after the CO_2RR for 1 h.

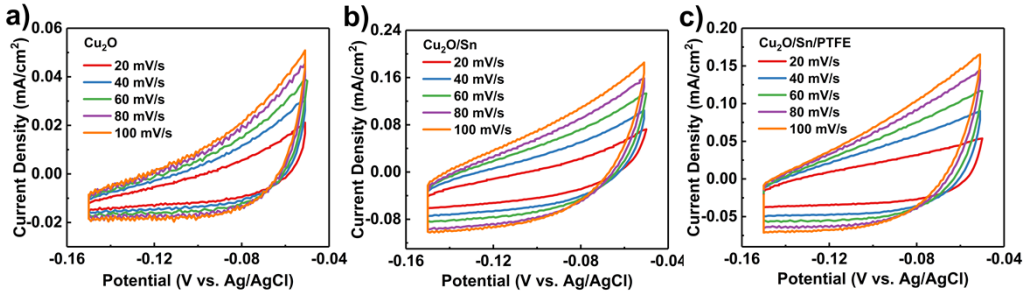

Figure S13. CV curves of the photocathodes a) Cu_2O, b) Cu_2O/Sn and c) Cu_2O/Sn/PTFE.

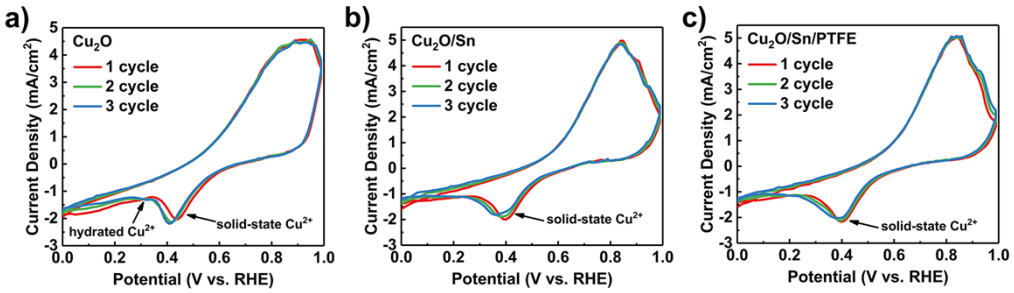

Figure S14. The CV curves of a) Cu_2O, b) Cu_2O/Sn and c) Cu_2O/Sn/PTFE under light in CO_2-saturated 0.1 M $KHCO_3$ aqueous solution.

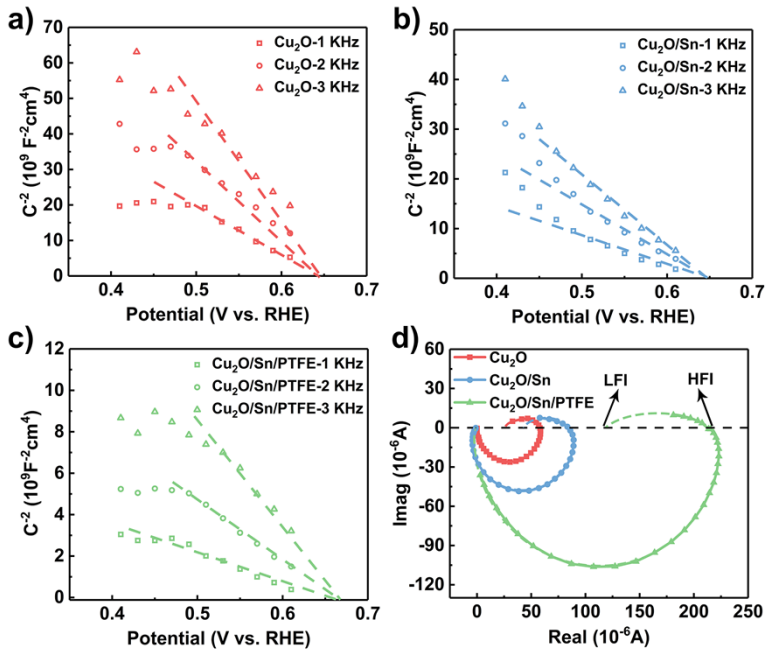

Figure S15. M-S plots measured at different frequencies for a) Cu_2O, b) Cu_2O/Sn and c) Cu_2O/Sn/PTFE. d) IMPS plots of Cu_2O, Cu_2O/Sn and Cu_2O/Sn/PTFE.

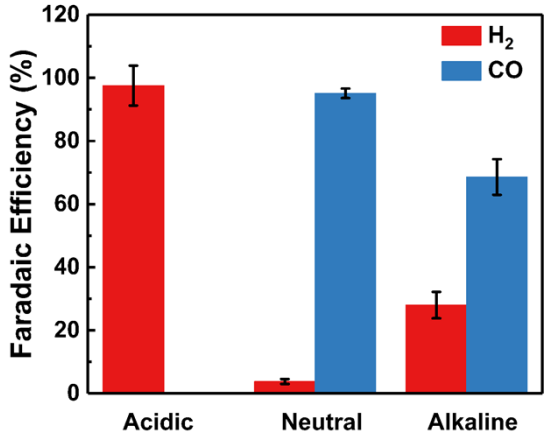

Figure S16. The product Faradaic efficiency of Cu_2O/Sn/PTFE at different pH electrolytes (-0.7 V vs. RHE).

Table S1. The contents of each component in Cu_2O/Sn/PTFE photoelectrode.

Elements	ICP-MS(wt. %)	XPS(Atomic (%))	Molar (%)
Cu	96.18	/	99.00 (Cu_2O)
Sn	0.79	44.44	0.87 (Sn)
F	/	13.38	0.13 (PTFE)

Table S2. Performance comparison of recent reports about Cu_2O photocathode for PEC CO_2RR.

Catalyst	Electrolyte	Potential	Products	FE	Ref.
Au/Cu_2O/AZO/TiO_2/ Re(4,4′-dimethylphosphonic acid-2,2′-bipyridine)$(CO)_3Cl$	AcCN/$TBAPF_6$	-2.05 V vs. Fc/Fc^+	CO	80%	1
$Cu_3(BTC)_2/Cu_2O$	AcCN/$TBAPF_6$	-1.77 V vs. Fc/Fc^+	CO	95%	2
Cu_2O/TiO_2/Re(tBu-bipy)$(CO)_3Cl$	AcCN/$TBAPF_6$	-1.73 V vs. Fc/Fc^+	CO	100%	3
Cu_2O/TiO_2-Cu^+	0.1 M $KHCO_3$	0.3 V vs. RHE	CH_3OH	50.7%	4
Cu_2O/In	0.1 M $KHCO_3$	-0.7 V vs. RHE	CO	81.8%	5
Cu_2O/SnO_x	0.5 M $NaHCO_3$	-0.35 V vs. RHE	CO	74%	6
Cu_2O/CuO/Pb	0.1 M KOH	-1.6 V vs. RHE	HCOOH, CH_3OH	40.45%	7
Cu_2O/Sn/PTFE	**0.1 M $KHCO_3$**	**-0.7 V vs. RHE**	**CO**	**95.1%**	**This work**

AcCN: acetonitrile;

$TBAPF_6$: tetrabutylammonium hexafluorophosphate.

Table S3. Physical resistance (R_1), charge transfer resistance (R_{ct}) and charge transfer efficiency of the photoelectrode.

Electrode	R_1/Ω	R_{ct}/Ω	Charge transfer efficiency/%
Cu_2O	24.33	32.63	47.0
Cu_2O/Sn	23.58	29.01	52.5
Cu_2O/Sn/PTFE	22.88	30.83	53.9

Reference:

1. M. Schreier, J. Luo, P. Gao, T. Moehl, M. T. Mayer and M. Grätzel, *J. Am. Chem. Soc.*, 2016, **138**, 1938-1946.
2. X. Deng, R. Li, S. Wu, L. Wang, J. Hu, J. Ma, W. Jiang, N. Zhang, X. Zheng, C. Gao, L. Wang, Q. Zhang, J. Zhu and Y. Xiong, *J. Am. Chem. Soc.*, 2019, **141**, 10924-10929.
3. M. Schreier, P. Gao, M. T. Mayer, J. Luo, T. Moehl, M. K. Nazeeruddin, S. D. Tilley and M. Grätzel, *Energy Environ. Sci.*, 2015, **8**, 855-861.
4. K. Lee, S. Lee, H. Cho, S. Jeong, W. D. Kim, S. Lee and D. C. Lee, *J. Energy Chem.*, 2018, **27**, 264-270.
5. Q. Wang, Y. Zhang, Y. Liu, K. Wang, W. Qiu, L. Chen, J. Li and W. Li, *Ind. Eng. Chem. Res*, 2022, **61**, 16470-16478.
6. Y. Zhang, D. Pan, Y. Tao, H. Shang, D. Zhang, G. Li and H. Li, *Adv. Funct. Mater.*, 2021, **32**, 2109600.
7. D. H. Won, C. H. Choi, J. Chung and S. I. Woo, *Appl. Catal. B*, 2014, **158-159**, 217-223.